ERL for Microfluorescence, Microspectroscopy and Microtomography

Mark Rivers
Center for Advanced Radiation Sources
The University of Chicago

Outline

- Advantages of ERL for fluorescence microbeam and microtomography techniques
- Considerations of bending magnets
- Challenges in optics and samples to take advantage of the ERL

Abstract

The ERL will be a tremendous advance over present storage ring sources for microprobe, microspectroscopy and microtomograpy applications. The increased brilliance can be used to increase the flux in a 1 micron spot by a factor of 100-1000, or to reduce the spot size to 100nm or less. The increased flux can be used to compensate for the low efficiency of high energy-resolution detectors required for many applications. It will also greatly increase the speed of fluorescence tomography experiments. The bending magnet sources at the ERL should not be neglected. High-field bending magnets on an ERL source would be ideal for 100 keV wide-fan beams for microtomography of large high-Z objects. Finally, the challenges in x-ray optics and radiation damage from an ERL source must be understood.

Smaller, More Intense Beams Obvious Advantages

- Brilliance-limited experiment
  - 1000x gain over APS if full brilliance can be utilized
  - 100x gain over APS certain (e.g. flux in 1 micron spot)
- 1 micron horizontal focus is difficult at APS
- Much easier with an ERL source, much less demagnification required
- Larger working distances will be available for installing good I_0 monitors
- Applications of micro-XRF, microspectroscopy
  - High pressure, diamond-anvil cell
  - Environmental science
  - Geochemistry, cosmochemistry
  - Materials science

High Energy-Resolution Detectors

- Need more intense beams
  - 10-100 times less solid angle than solid state detectors
- Wavelength dispersive spectrometers
  - Required for many experiments with spectral overlaps or major element fluorescence
- High-resolution emission spectroscopy
  - Spin-state studies at high pressure

Kβ emission spectra of Fe_2O_3 at 1 at 72 GPa,
(C. Kao, NSLS, Brookhaven National Lab.)

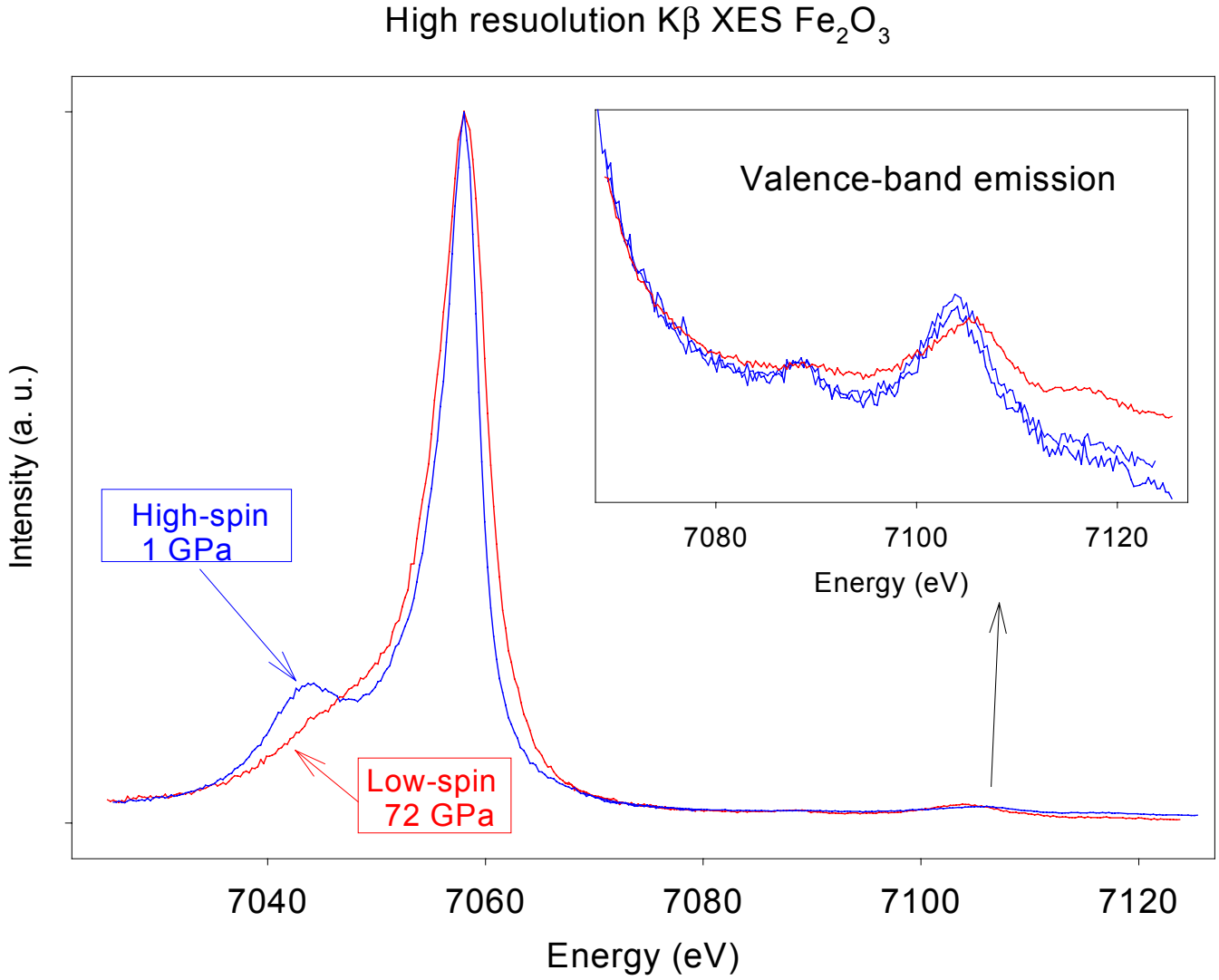

High-resolution Rowland Circle Spectrometer

(C. Kao, NSLS, Brookhaven National Lab.)

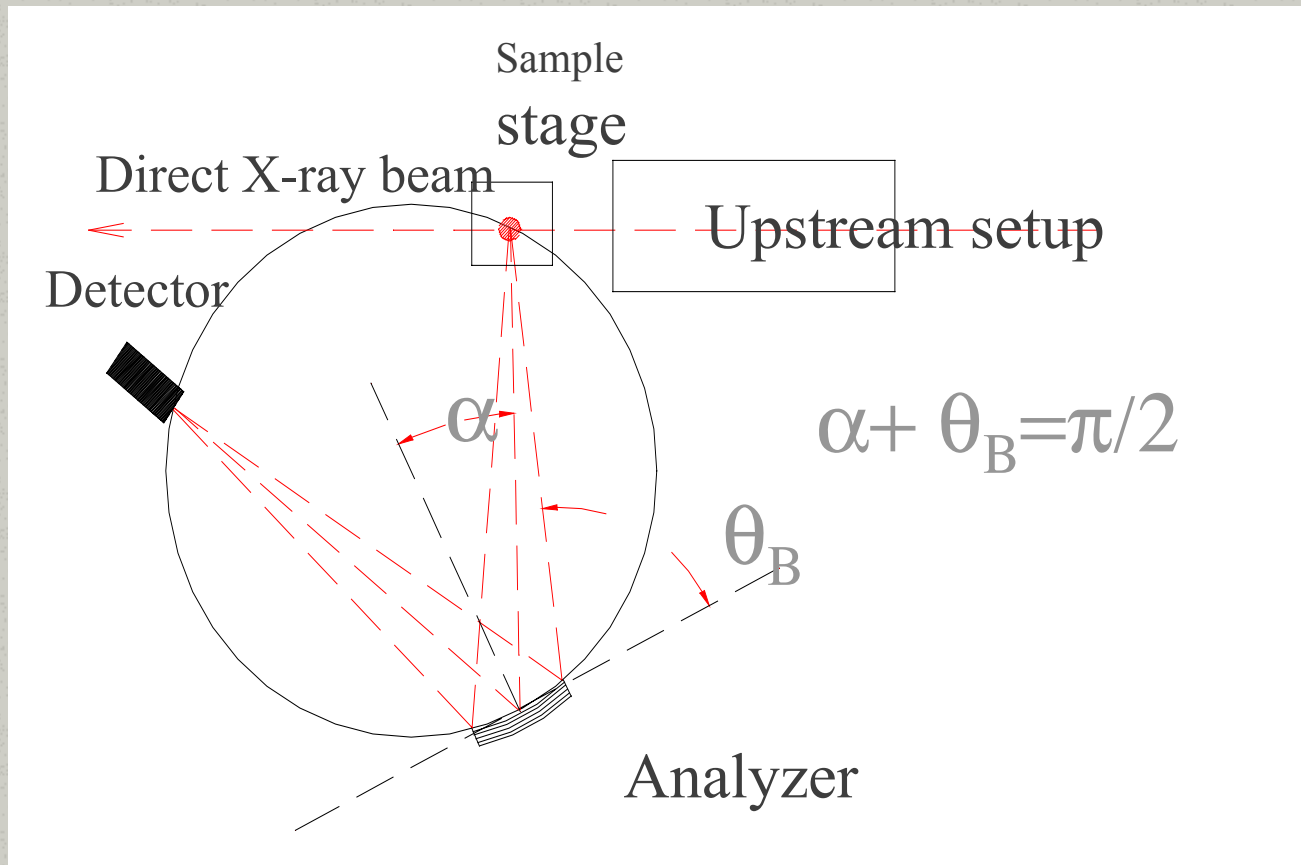

Fluorescence Microtomography

- Best way to get trace element distribution in 3-dimensions for fragile samples
- Requires first-generation computed-tomography techniques, e.g. 3-D mechanical scanning
- Want very high count rates to perform data collection in reasonable time
- Hours at APS becomes minutes at ERL

Computed Microtomography

- Transmission computed tomography can benefit from 3 aspects of ERL source
- Increased coherence of the source for phase contrast imaging
- Increased flux in transmitted beam
- Much higher flux at very high energy???

Bending Magnets

- ERL does not require low-field bending magnets to reduce emittance
- ERL does not require symmetry, bends can have different fields
- NSLS x-ray bends have 1.25 Tesla field
- 1.25 Tesla field on ERL is 40 keV critical energy
- Brightness (not brilliance) is ~10X greater than APS bending magnet at 100 keV, ~100X at 200 keV
- High-energy applications
  - Microtomography
  - High-pressure diffraction in the multi-anvil press

Challenges

- Sub-microradian slope errors on K/B mirrors
  - However, even if we can't take full advantage of the smaller source size the smaller divergence puts a lot more photons in a 1 micron spot with proven optics
- Thickness effects in samples to take advantage of sub-micron spatial resolution – hard to make real samples thin enough to avoid 3-D depth problems
- Ultimate limits due to secondary electrons, path lengths ~1 micron for 10 keV electrons
- Radiation damage
  - At APS photochemistry is a already problem for non-biological samples especially if wet

Microfluorescence Imaging and Tomography

Matt Newville, Steve Sutton, Mark Rivers, Peter Eng
GSECARS, Sector 13, APS
The University of Chicago

- GSECARS beamline and microprobe station, Kirkpatrick-Baez mirrors
- 2 dimensional elemental mapping
- 2 dimensional oxidation state mapping
- x-ray fluorescence tomography

The GSECARS Fluorescence Microprobe Station

The GeoSoilEnviroCARS beamline 13-IDC provides a micro-beam facility for x-ray fluorescence (XRF) and x-ray absorption spectroscopy (XAS) studies in earth and environmental sciences.

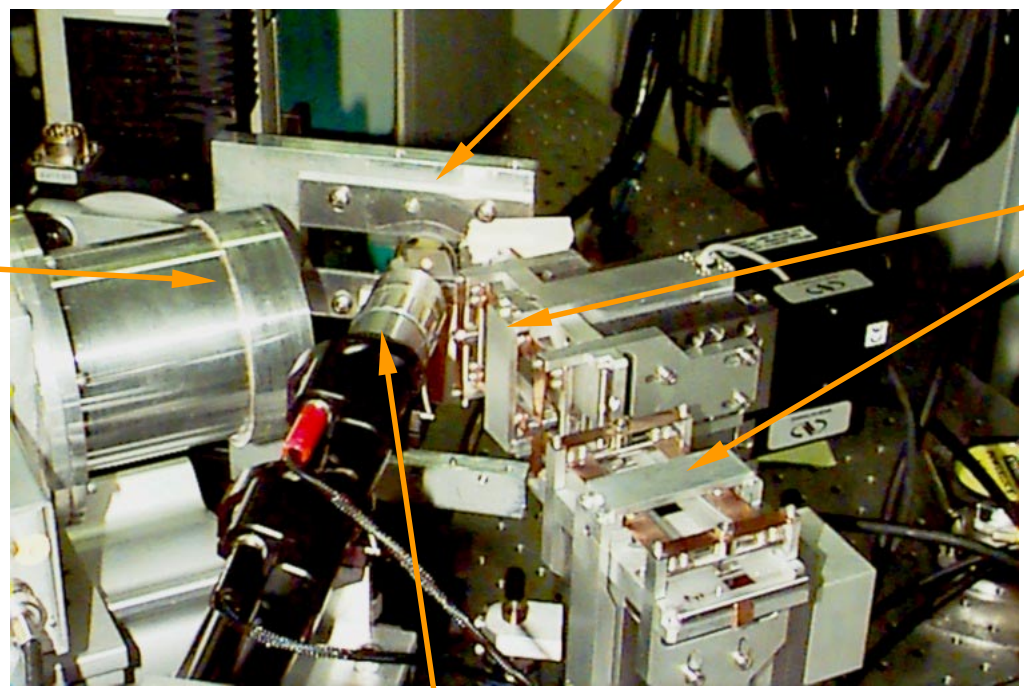

Kirkpatrick-Baez focusing mirrors

The table-top Kirkpatrick-Baez mirrors use a four-point bender and a flat, trapezoidal mirror to dynamically form an ellipsis. They can focus a 300x300μm monochromatic beam to 1x1μm - a flux density gain of 10^5.

With a typical working distance of 100mm, and an energy-independent focal distance and spot size, they are ideal for micro-XRF and micro-EXAFS.

We routinely use Rh-coated silicon (horizontal) and fused-silica (vertical) mirrors to produce 4x4μm beams for XRF, XANES, and EXAFS.

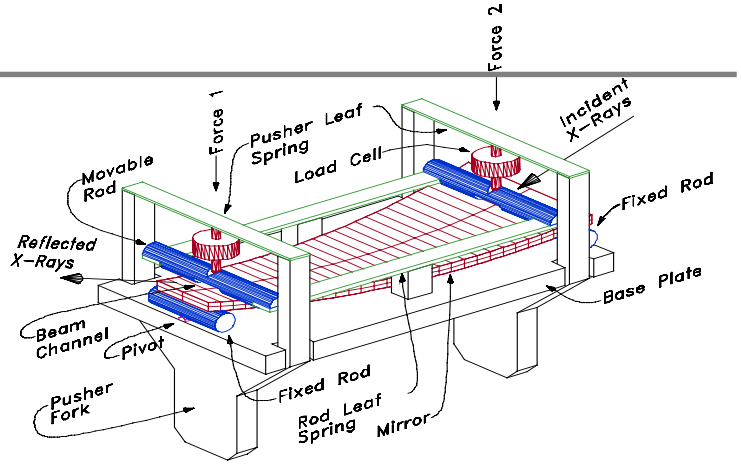

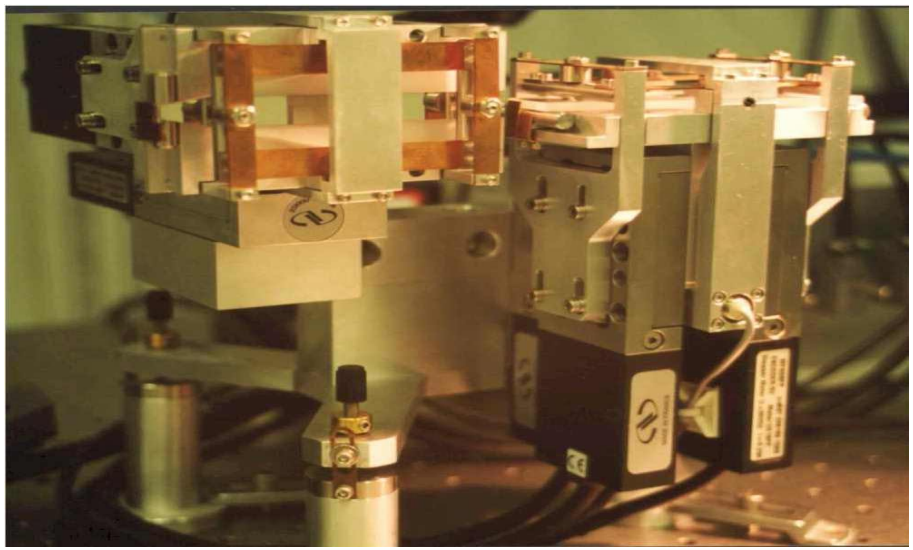

Double Focused Undulator Beam
Flux Density Gain = 113,000

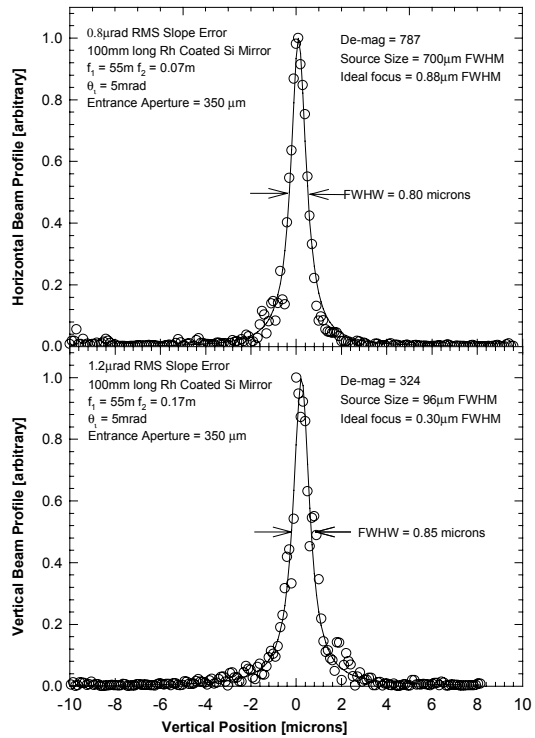

X-ray Fluorescence Microprobe

Experiment: Measure characteristic x-ray emission lines from de-excitation of electronic core levels for each atom.

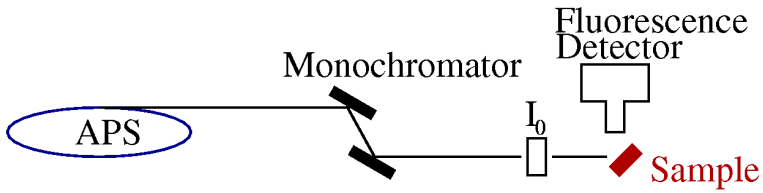

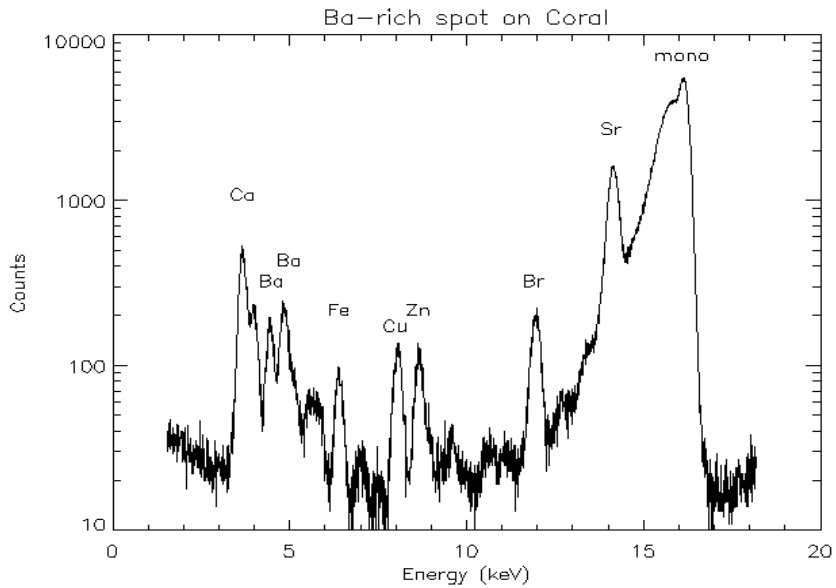

Key Attributes:

Element Specific: all elements (with Z>16 or so) can be seen at the APS, and it is usually easy to distinguish different elements.

Quantitative: relative abundances of elements can be made with high precision and accuracy. x-ray interaction with matter well understood.

XANES/XAFS/XRD combination: can be combined with other x-ray micro-techniques to give complementary information on a sample

Low Concentration: concentrations down to a few ppm can be seen.

Natural Samples: samples can be in solution, liquids, amorphous solids, soils, aggregates, plant roots, surfaces, etc.

Small Spot Size: measurements can be made on samples down to a few microns in size.

X-ray Fluorescence detector: Solid-State Ge Detector

Ge solid-state detectors give energy resolutions down to ~250 eV to separate fluorescence from different elements, and allow a full fluorescence spectrum (or the windowed signal from several elements) to be collected in seconds.

Ge detectors are also limited in ***total count rate*** (up to ~100KHz), so multiple elements (~10) are used in parallel.

Using such detectors gives detection limits at or below the ppm level, and allows XANES and EXAFS measurements of dilute species in heterogeneous environments.

2D XRF Mapping: Pu sorbed toYucca Mountain Tuff

Martine Duff, Doug Hunter, Paul Bertsch (Savannah River Ecology Lab, U Georgia)
Matt Newville, Steve Sutton, Peter Eng, Mark Rivers (Univ of Chicago)

A natural soil sample from the proposed Nuclear Waste Repository at Yucca Mountain, NV, was exposed to an aqueous solution of ^{239}Pu (~1μM).

Fluorescence Maps of 150μm X 150μm areas were made with a 4x7μm x-ray beam from the GSECARS microprobe. Mn, Fe, As, Pb, Sr, Y, and Pu fluorescence were measured simultaneously using a solid-state (Si/Li) detector.

The Pu was seen to be highly correlated with Mn-rich minerals in the zeolite- and quartz-rich material, and not with the zeolites, quartz, or Fe-rich minerals.

XANES and EXAFS measurements were made at the Pu L_{III} edge of "hot spots" A1 and A2 ….

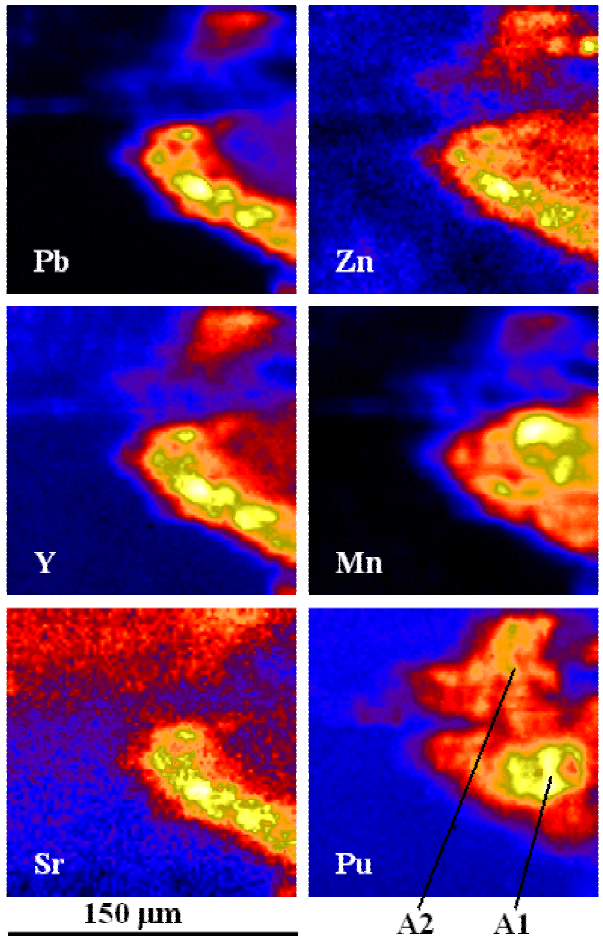

XANES and EXAFS: Pu sorbed to Yucca Mountain Tuff

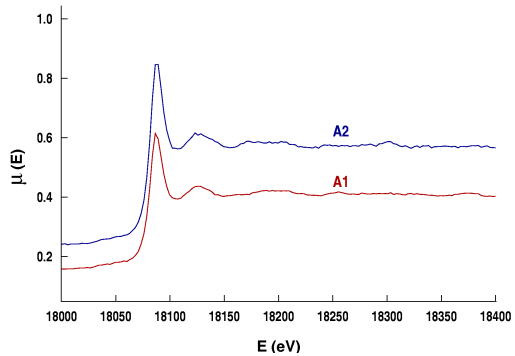

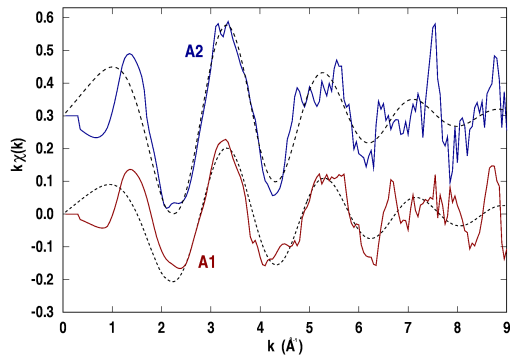

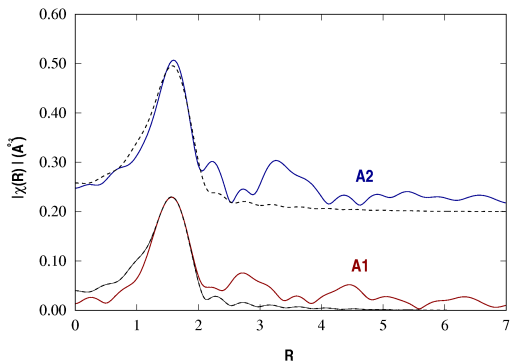

XANES features showed the Pu to be in either Pu^{4+} or Pu^{5+} (or a mixture of the 2) but not Pu^{6+}. Further measurements (planned for Fall 1999) should help distinguish these two states.
Since the initial Pu solution had Pu^{5+} and since the Mn-rich minerals were dominated by Mn^{4+}, both are plausible.

The Extended XAFS (with oscillations isolated from atomic-like background, and then Fourier transformed to show a radial distribution function) shows Pu coordinated by 6--8 oxygens at ~2.26A in the first shell, consistent with Pu^{4+} or Pu^{5+} (but again not Pu^{6+}).
No reliable second shell could be seen from this data, probably indicating several different Mn second shell distances -- the Pu appears to be weakly bound to the disordered Mn minerals (more measurements needed).

Low Concentration/Small Spot XRF Maps: Pb sorbed to alumina/biofilm

A. Templeton, G. E. Brown, Jr. (Stanford Univ)

Microscopic organisms in natural systems can alter the chemical and physical state of mineral-water interfaces. It is likely that sorption properties of metal ions is dramatically altered by the presence of microbial biofilms.

Pb sorbed onto a biofilm of the bacterium *Burkholderia cepacia* grown on an α-Al_2O_3 was studied by mapping the distribution of Pb sorbed to biofilm-coated minerals, so as to correlate Pb-speciation from bulk XANES/EXAFS (from SSRL) with location (mineral surface, cells, etc).

Due to the very low Pb concentrations and small features, high-quality fluorescence micro-XAFS from these samples is quite challenging, but possible.

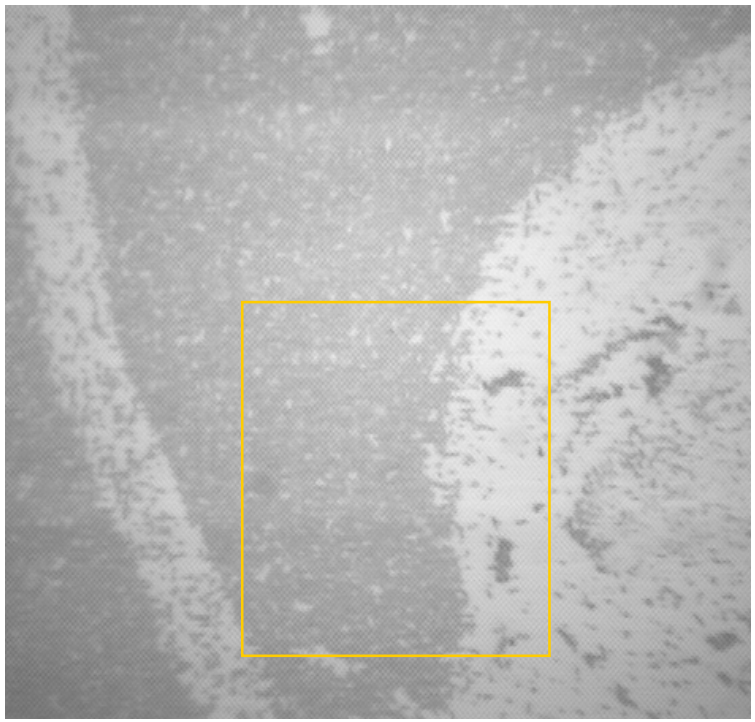

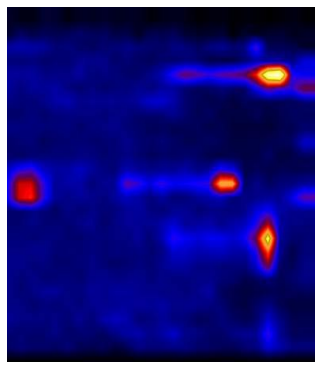

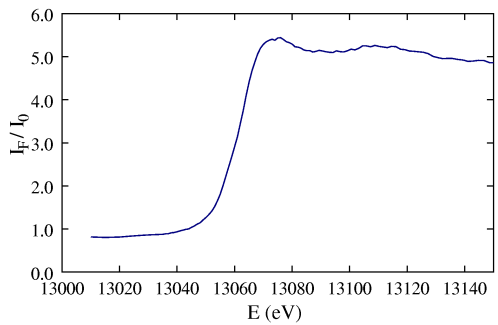

Oxidation state maps: Mn redox at plant roots and hyphae

D. Schulze (Purdue Univ)

Manganese is an essential nutrient in plants, needed for physiological processes including photosynthesis and for response to stress and pathogens. Reduced Mn^{2+} is soluble and bio-available in soils, but oxidized Mn^{4+} precipitates (along with Mn^{3+}) as insoluble Mn oxides. The redox chemistry of Mn in soil is complex, with both reduction and oxidation catalyzed by microorganisms.

Spatially-resolved, micro-XANES is well-suited for mapping Mn oxidation state in live plant rhizospheres in an attempt to better understand the role of Mn redox reactions in a plant's ability to take up toxic trace elements.

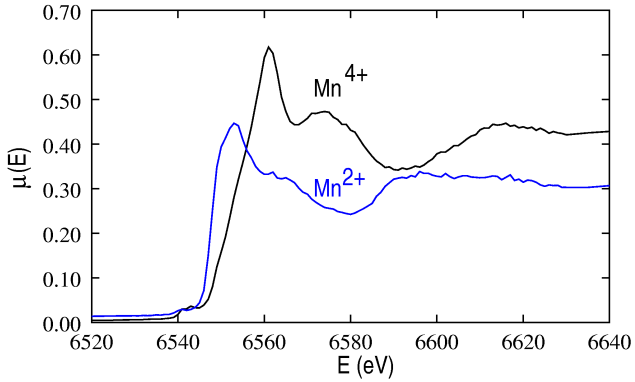

Collecting Mn fluorescence at selected incident energies around the Mn K-edge, we can make 3-d (X-Y-E) maps that give the spatial distribution of different Mn valence states.

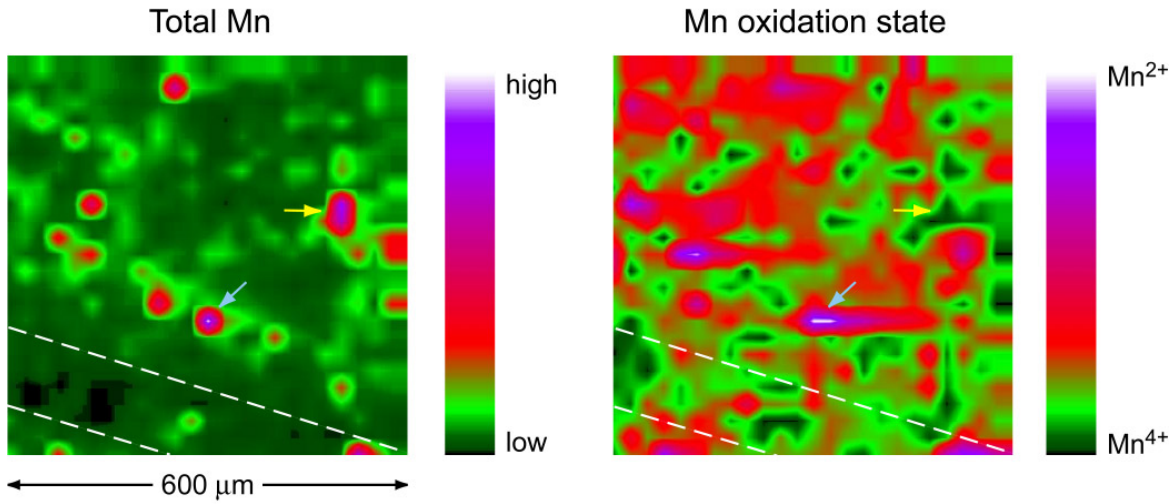

XRF image of total Mn concentration (left) of soil traversed by a sunflower root (dashed line) showing the heterogeneous distribution of Mn, with enrichment near the root. The Mn oxidation state map of this same region (right) shows both Mn^{2+} and Mn^{4+} in the Mn-rich sites, with a tendency for the reduced species to concentrate near the root.

Detector Resolution: Solid State Detectors Revisited

The energy resolution of solid-state detectors (200 eV at best, often limited to count rates to ~1KHz), is sometimes not good enough -- especially with heterogeneous samples with many nearby fluorescence lines.

Solid state detectors are also limited in ***total count rate*** (up to ~100KHz per element, but at the worst resolution), which can be a problem -- especially with intense x-ray beams.

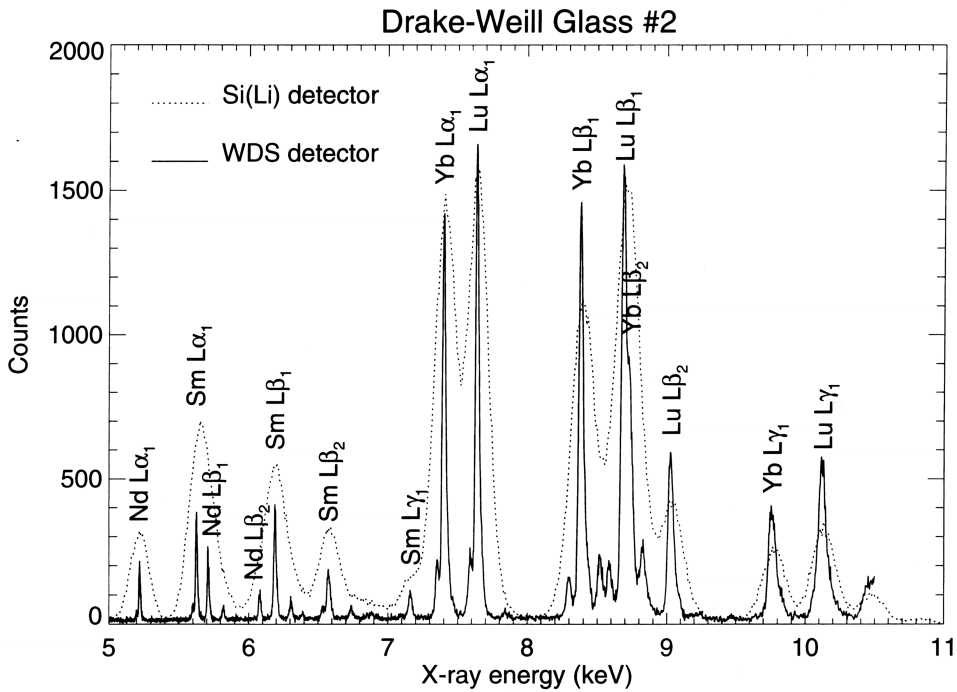

XRF spectra for a synthetic glass containing several rare-earth elements using both a Si(Li) detector and a Wavelength Dispersive Spectrometer. Data collected at NSLS X-26A, Steve Sutton and Mark Rivers.

Wavelength Dispersive Spectrometer (WDS)

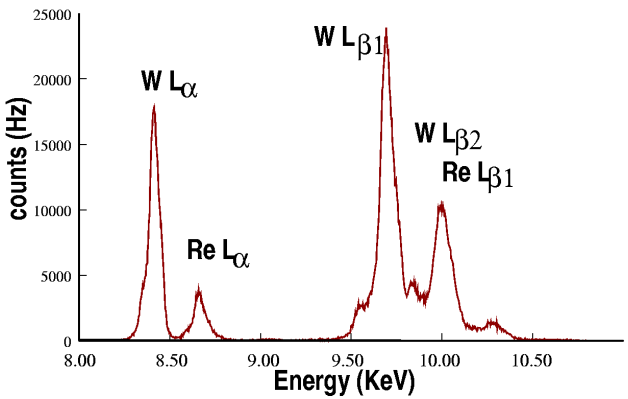

The Wavelength Dispersive Spectrometer uses an analyzer crystal on a Rowland circle to select a fluorescence line. This has much better resolution (down to ~30eV) than a solid state detector (~250eV), doesn't suffer dead-time from electronics, and often has superior peak-to-background ratios. The solid-angle and count-rates are lower, and multiple fluorescence lines cannot be collected during mapping.

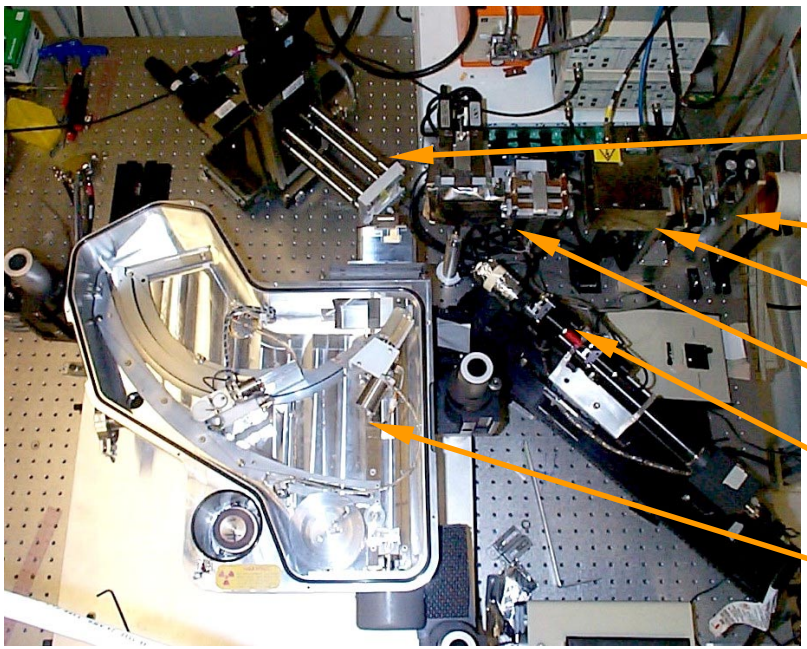

Sample and x-y-z stage

Table-top slits

Ion chamber

Kirkpatrick-Baez focusing mirrors

Optical microscope

Wavelength Dispersive Spectrometer

Using the WDS for XRF Mapping: Cs on biotite

J. McKinley, J. Zachara, S. M. Heald (PNNL)

Biotitie is a mica that contains trace amounts of many transition metals, a few percent Ti, and major components of Ca and Fe. To study how Cs would bind to the surface and inner layers of biotite, McKinley and Zachara exposed natural mica to a Cs-rich solution, embedded the mica in epoxy resin and cut cross-sections through the mica.

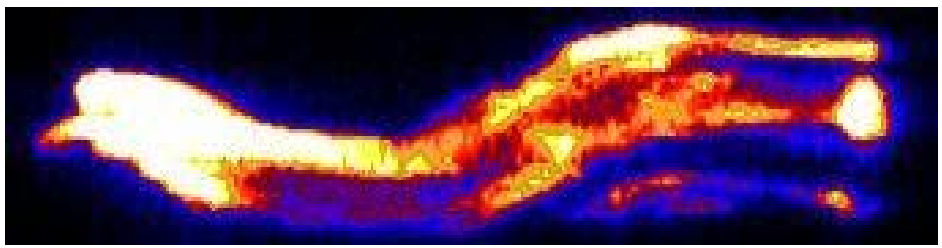

1000 x 200μm image of the Cs L_α line in biotite with a 5x5μm beam, 5μm steps and a 2s dwelltime at each point. The incident x-ray energy was 7KeV.

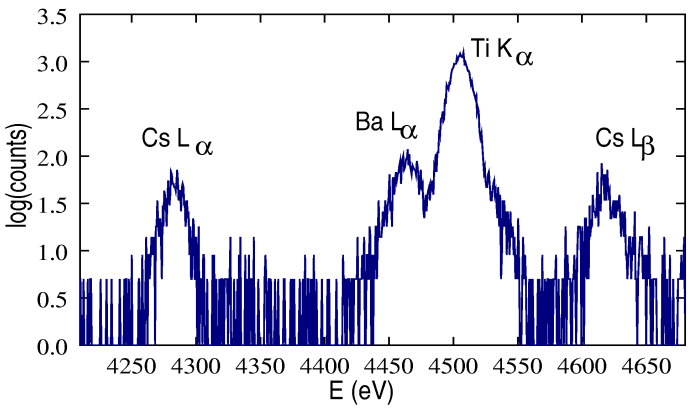

Detecting the Cs L_α fluorescence line is complicated by the nearby Ti K_α line. A high resolution fluorescence detector such as the WDS can make this easier.

Using the WDS for XRF/XANES: 1000ppm Au in FeAsS

Louis Cabri (NRC Canada), Robert Gordon, Daryl Crozier (Simon Fraser), PNC-CAT

1000ppm Au in FeAsS (arsenopyrite): The understanding of the chemical and physical state of Au in arsenopyrite ore deposits is complicated by the proximity of the Au L_{III} and As K edges and their fluorescence lines.

At the Au L_{III}-edge, As will also be excited, and fluoresce near the Au L_{α} line. Even using the WDS, the tail of the As K_{α} line persists down to the Au L_{α} line, and is still comparable to it in intensity.

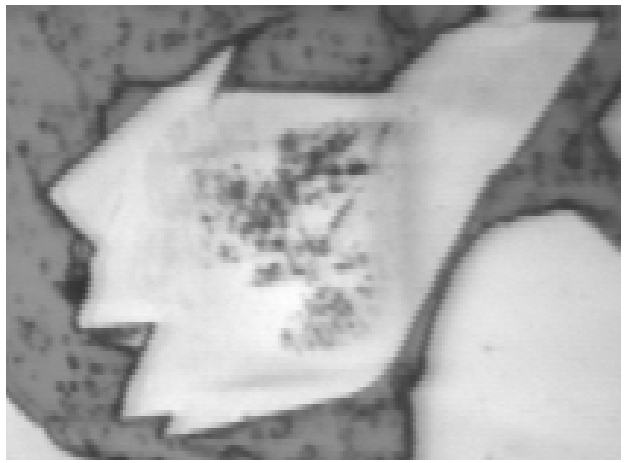

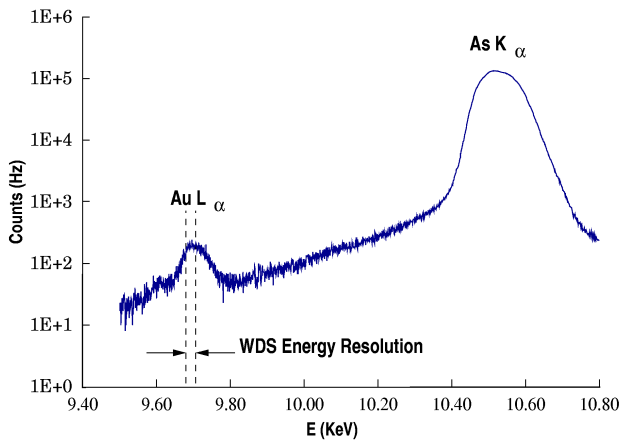

250x250µm image of the Au L_{α} line in arsenopyrite with a 6x6µm beam, 5µm steps and a 2s dwell time at each point. The x-ray energy was 12KeV.

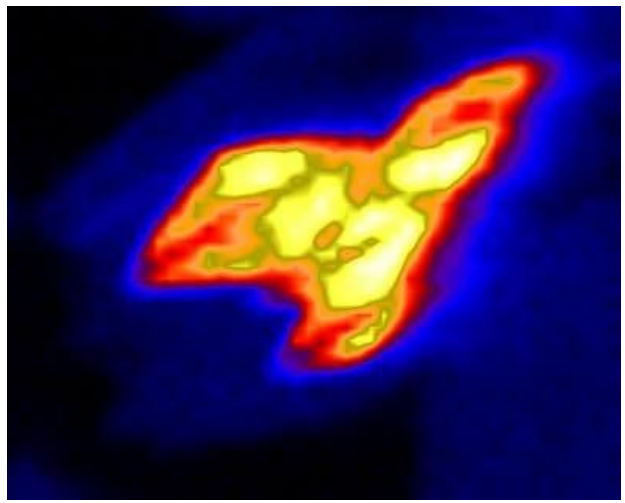

Using the WDS for XANES: 1000ppm Au in FeAsS

Louis Cabri (NRC Canada), Robert Gordon, Daryl Crozier (Simon Fraser), PNC-CAT

The tail of the As K_α line is still strong at the Au L_α energy, so using a Ge detector gave the Au L_{III} edge-step as about the same size as the As *K* edge-step, and the Au XANES was mixed with the As EXAFS.

With the WDS, the As edge was visible, but much smaller, and so the Au XANES was clearer.

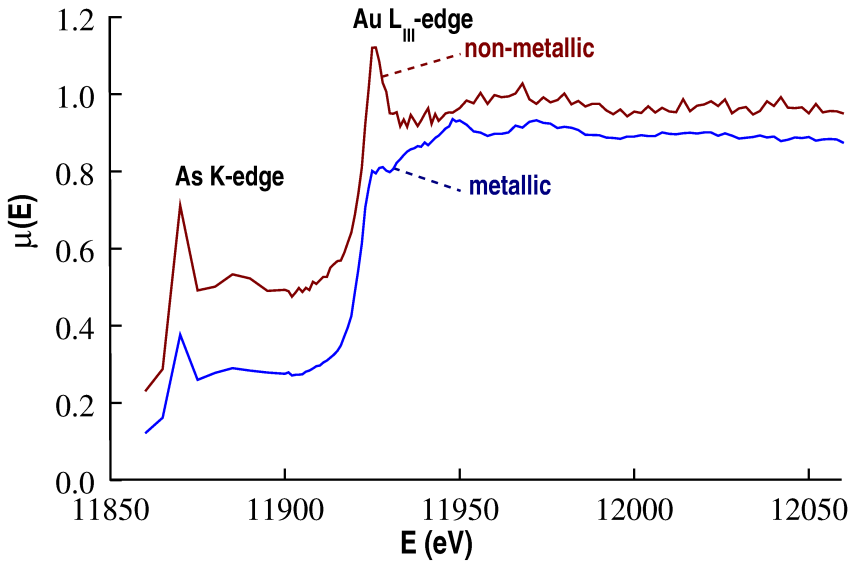

As *K*-edge	11.868 KeV
As K_α line	10.543 KeV
Au L_{III}-edge	11.918 KeV
Au L_α line	9.711 KeV

The Au L_{III} edge of two different natural samples of FeAsS with the WDS. Both samples had ~1000ppm of Au. We see clear evidence for metallic and oxidized Au in these ore deposits.

Fluorescence Tomography: Overview

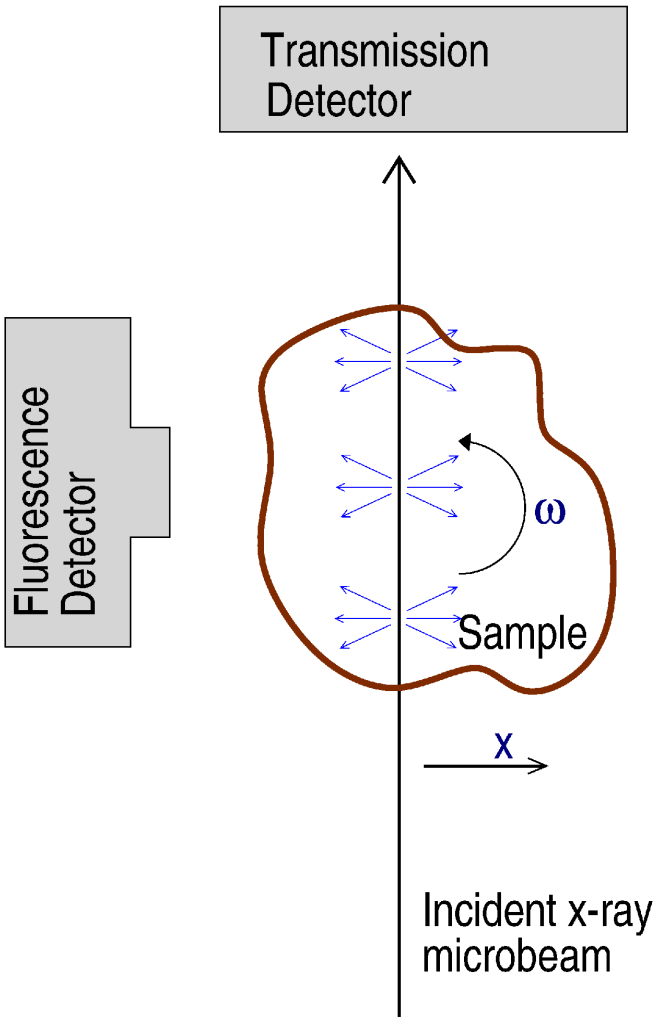

Conventional x-ray computed microtomography (CMT) provides 3D images of the x-ray attenuation coefficient within a sample using a transmission detector. Element-specific imaging can be done by acquiring transmission tomograms above and below an absorption edge, or by collecting the characteristic fluorescence of the element.

Fluorescent x-ray tomography is done as first-generation mode tomography, using a ***pencil-beam*** scanned across the sample for several angular setting. The sample is rotated around **ω**, and the scan of **x** is repeated. Transmission x-rays are can be measured as well to give an overall density.

Characteristics:

- can collect multiple fluorescence lines at a time.
- data collection is relatively slow.
- fluorescence can be complicated by self-absorption.
- sample size limited by total absorption length .

Fluorescence Tomography: Experimental Setup

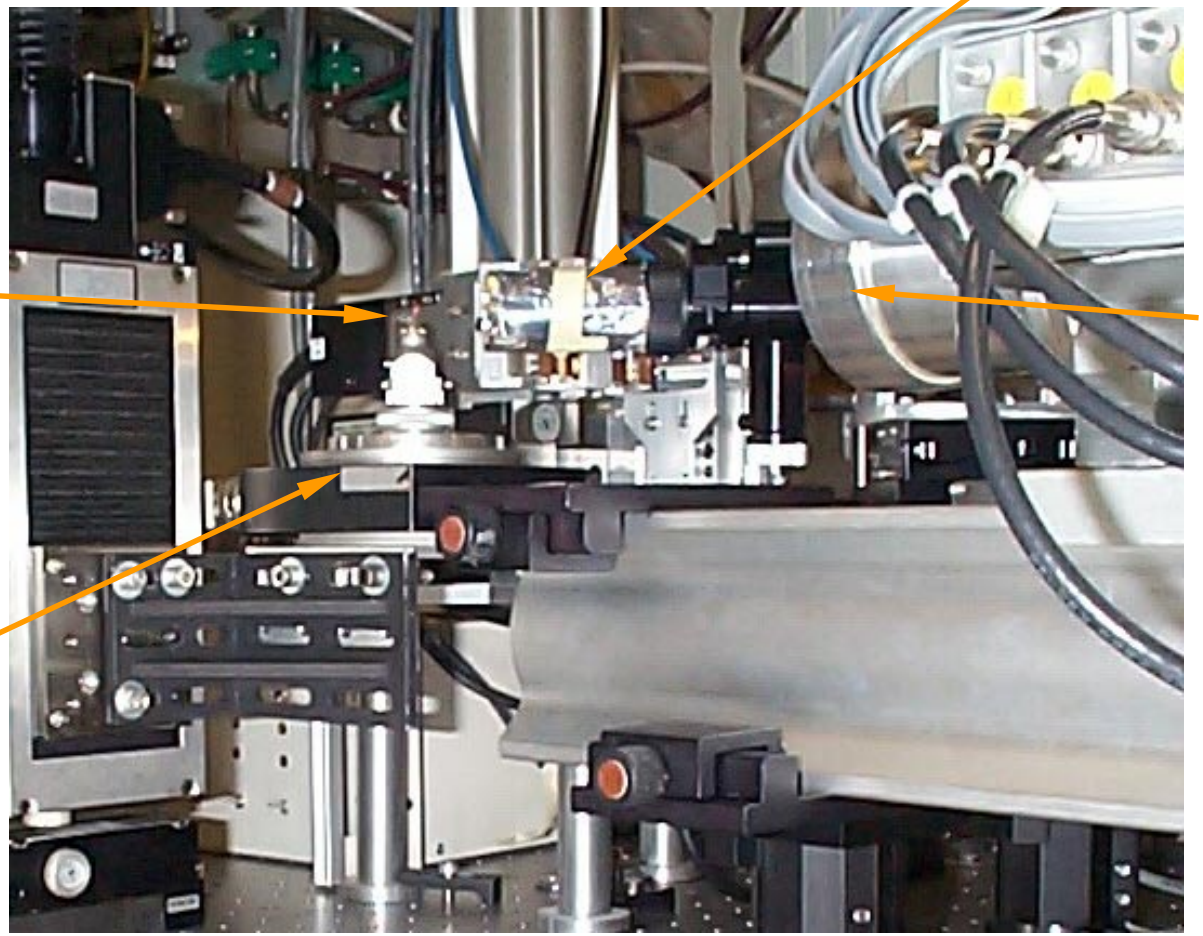

Fluorescence Tomography: Sinograms

The Raw fluorescence tomography data consists of elemental fluorescence (uncorrected for self-absorption) as a function of position and angle: a ***sinogram***. This data is reconstructed as a virtual ***slice*** through the sample by a coordinate transformation of (x,ω) -> (x, y). The process can be repeated at different z positions to give three-dimensional information.

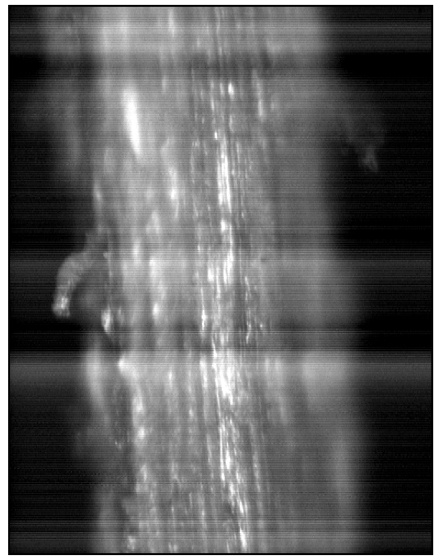

Fluorescence Sinograms for Zn, Fe, and As collected simultaneously for a section of contaminated root (photo, right):

x: 300µm in 5µm steps **ω**: 180° in 3° steps

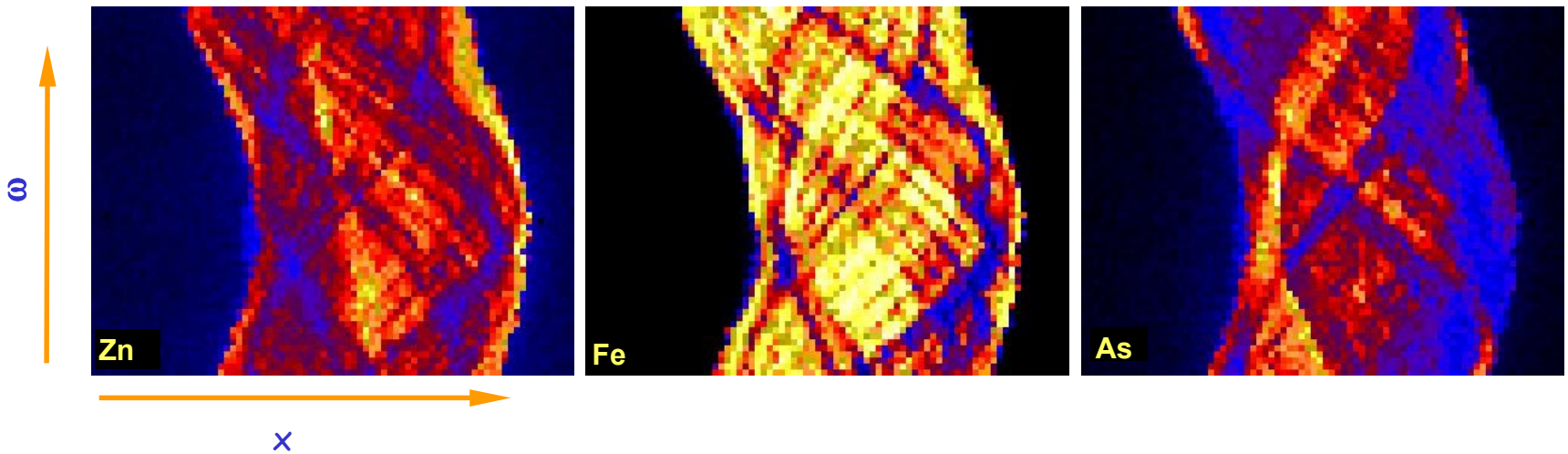

Fluorescence Tomography: Distributions of Heavy Metals in Roots

S. Fendorf, C. Hansel (Stanford): **Toxic Metal Attenuation by Root-borne Carbonate Nodules**

The role of root-borne carbonate nodules in the attenuation of contaminant metals in aquatic plants is being investigated using a combination of EXAFS, SEM, X-ray microprobe and fluorescence CT. The CT images of a 300 micron root cross section (*Phalaris arundinacea)* shows Fe and Pb uniformly distributed in the root epidermis whereas Zn and Mn are correlated with nodules. Arsenic is highly heterogeneous and poorly correlated with the epidermis suggesting a non-precipitation incorporation mechanism.

Such information about the distribution of elements in the interior of roots is nearly impossible to get from x-y mapping alone:

Physically slicing the root causes enough damage that elemental maps would be compromised.

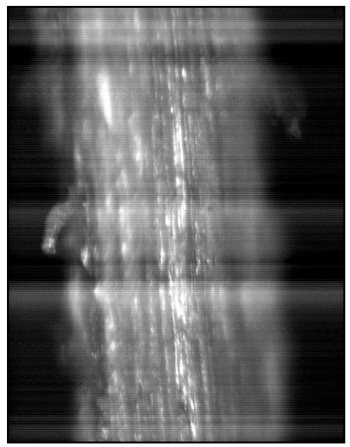

photograph of root section and reconstructed slices of fluorescent x-ray CT for selected elements.

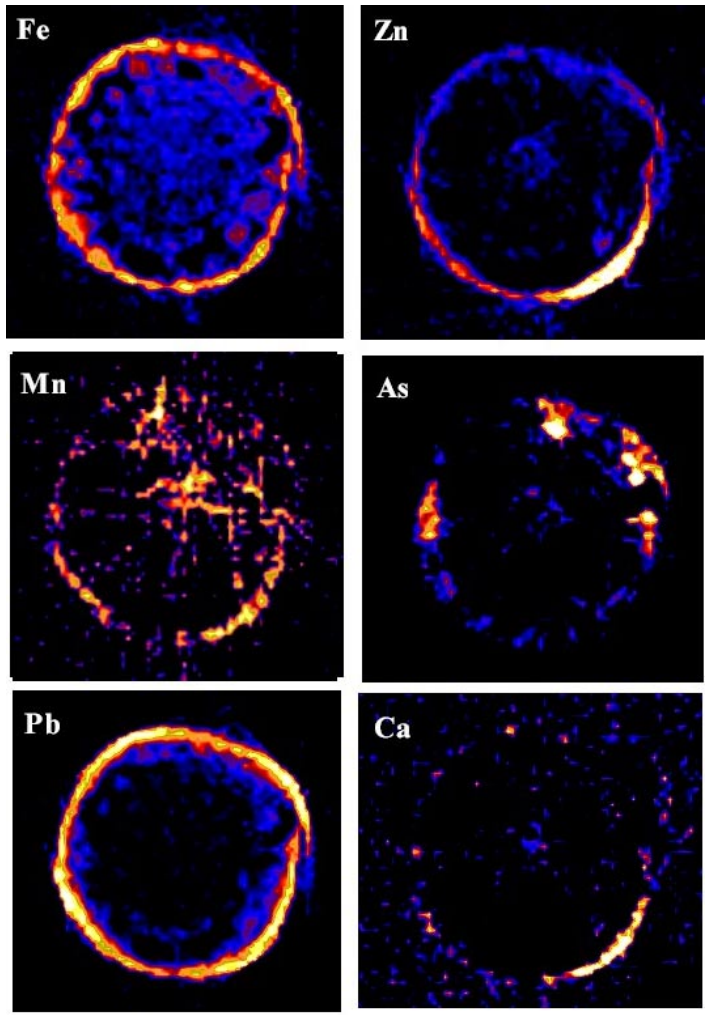

Fluorescence Tomography: Interplanetary Dust Particles

G. J. Flynn (SUNY, Plattsburgh): **Volatile elements in interplanetary dust**

Interplanetary Dust Particles (IDPs) collected by NASA aircraft from the Earth's stratosphere allow laboratory analysis of asteroidal and cometary dust.

MicroXRF analyses show enrichment of volatile elements, suggesting the particles derive from parent bodies more primitive than carbonaceous chondrites (Flynn and Sutton, 1995). The IDP fluorescence tomography images show that volatile elements (Zn and Br) are not strongly surface-correlated, suggesting that these elements are primarily indigenous rather than from atmospheric contamination

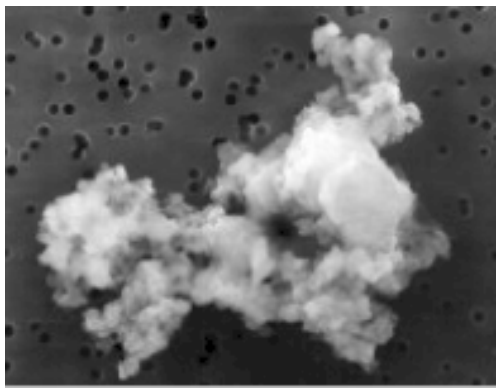

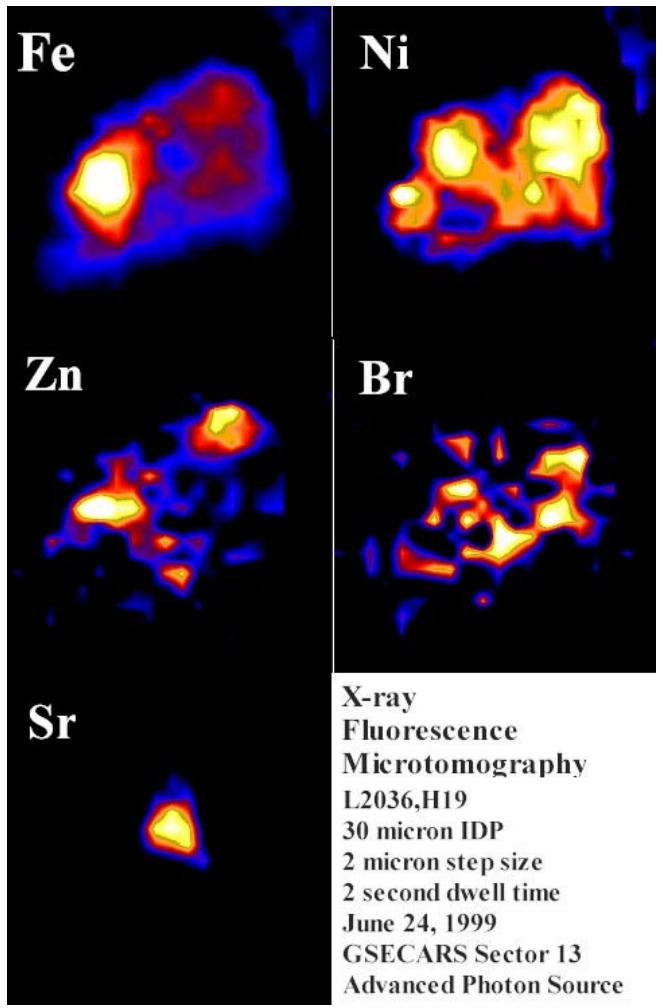

Fluorescence Tomography: Trace Elements in Goffs Pluton Zircons

M. McWilliams (Stanford Univ)

Fluorescence CT of individual zircon crystals shows the heterogeneities of U, Th, and Y in candidate crystals for U-Pb dating. Zircons from Goffs Pluton (Mojave) have Proterozoic cores and Cretaceous overgrowths. The tomography images for a 150 µm zircon show that the overgrowths are associated with U and Th enrichment. The crystal contains a large void (dark triangular feature). There is also some U and Th "mineralization" within the void that is zirconium-free (compare U and Zr images). The yttrium distribution is quite heterogeneous with a tendency of anti-correlation with Zr, U and Th.

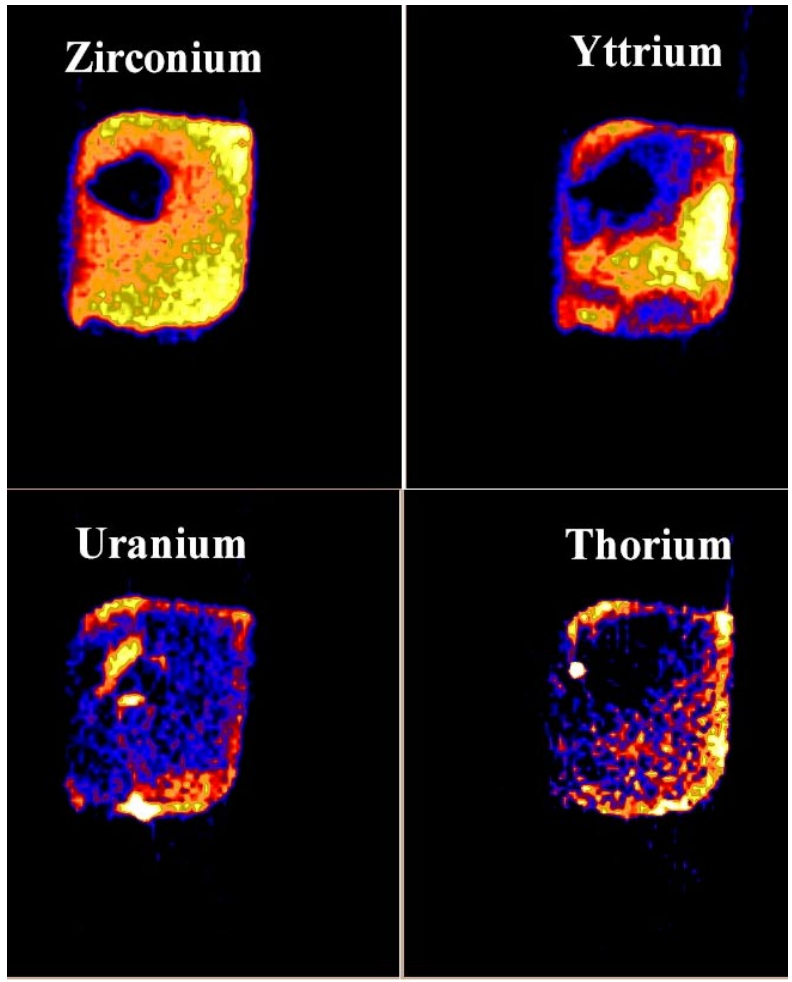

Fluorescence CT in such a strongly absorbing sample (nearly all Zr!) is complicated by self-absorption. These reconstructions are the result of a crude correction for self-absorption in the sinograms.

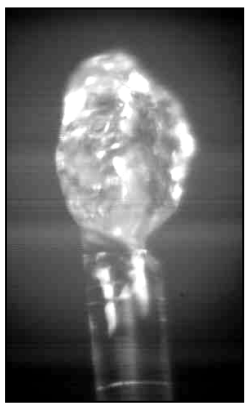

Fluorescence Tomography: Self Absorption in Zr sinogram

Uncorrected sinogram (detector viewing from the right) for Zr fluorescence of $ZrSiO_4$. There is significant self-absorption.

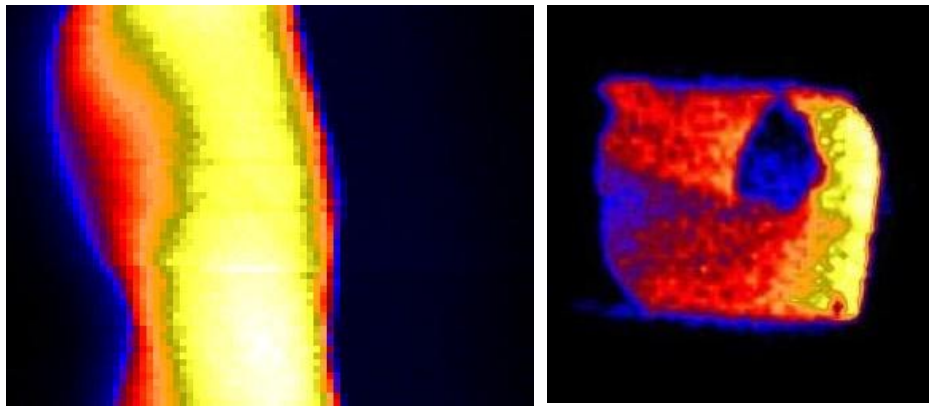

The simplest self-absorption correction to the sinogram uses a uniform absorption coefficient of the sample, and does a row-by-row correction. This gives a more uniform density across the sinogram and the reconstructed slice.

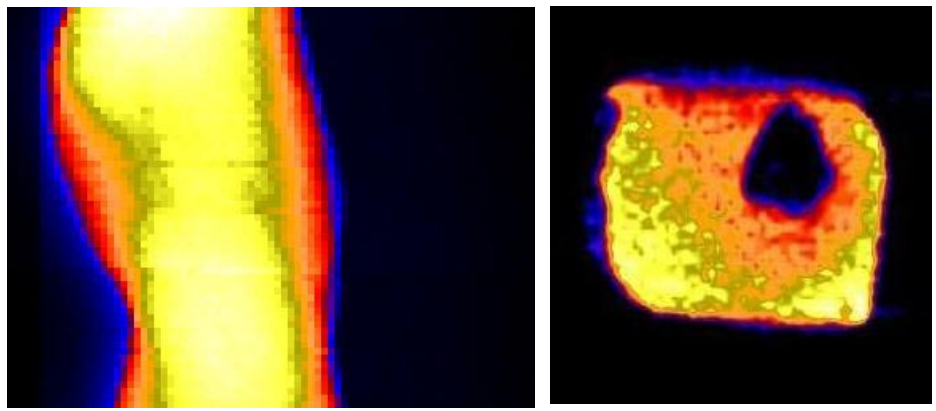

Sinograms and reconstructed slices for Zr fluorescence from zircon: uncorrected (top) and corrected (bottom) for self-absorption.

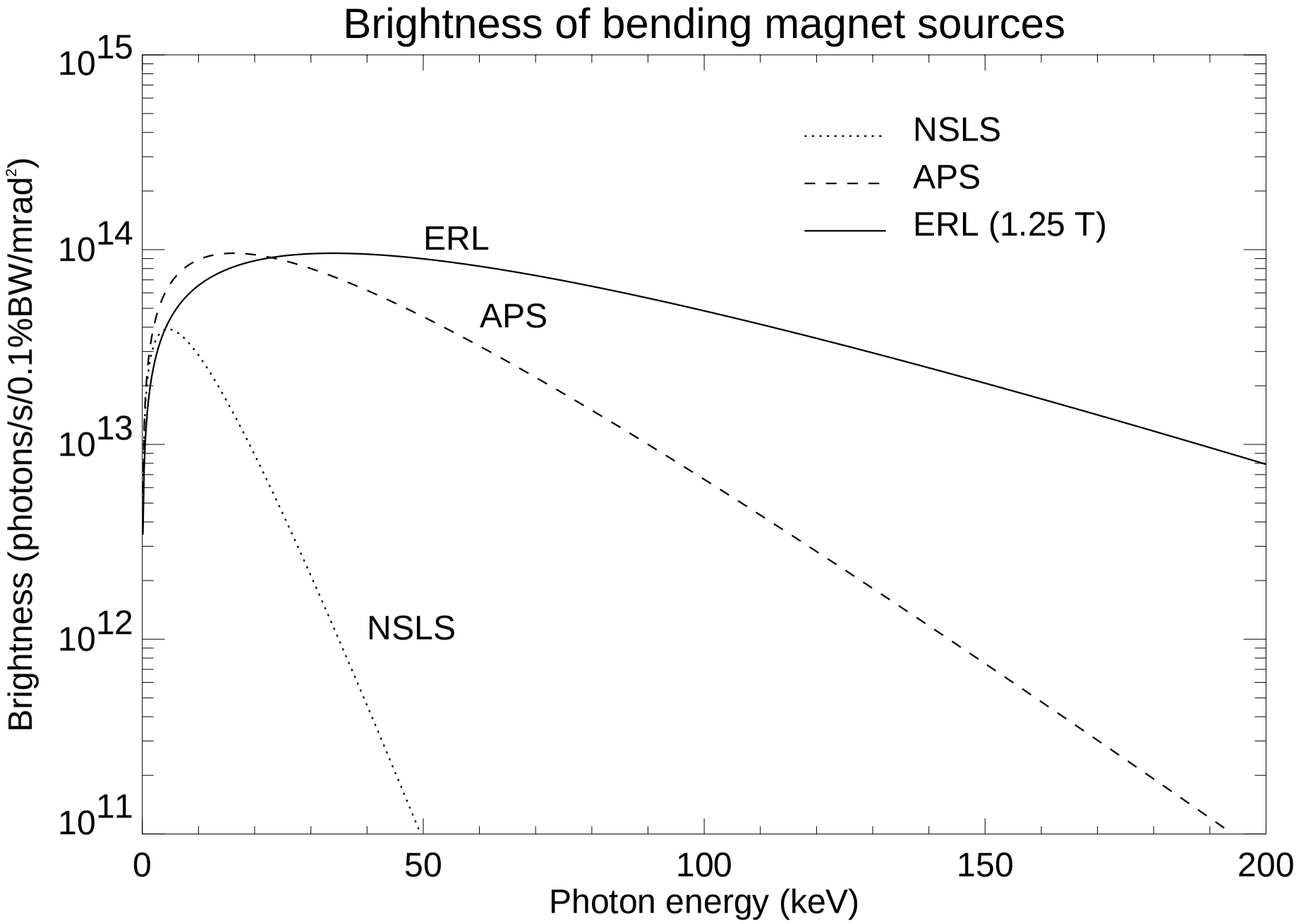
Brightness of bending magnet sources
NSLS
APS
ERL (1.25 T)
ERL
APS
NSLS
Brightness (photons/s/0.1%BW/mrad²)
Photon energy (keV)
10¹⁵
10¹⁴
10¹³
10¹²
10¹¹
0
50
100
150
200